Development of a Scaled Vehicle With Longitudinal Dynamics of an HMMWV for an ITS Testbed

Rajeev Verma, *Student Member, IEEE*, Domitilla Del Vecchio, and Hosam K. Fathy

***Abstract*—This paper applies Buckingham's π theorem to the problem of building a scaled car whose longitudinal and powertrain dynamics are similar to those of a full-size high-mobility multipurpose wheeled vehicle (HMMWV). The scaled vehicle uses hardware-in-the-loop (HIL) simulation to capture some of the scaled HMMWV dynamics physically, and simulates the remaining dynamics onboard in real time. This is performed with the ultimate goal of testing cooperative collision avoidance algorithms on a testbed comprising a number of these scaled vehicles. Both simulation and experimental results demonstrate the validity of this HIL-based scaling approach.**

***Index Terms*—Buckingham's π theorem, drivetrain, hardware-in-the-loop (HIL).**

NOMENCLATURE

$\rho_{\rm air}$	Air density (kg/m^3).
g	Acceleration due to gravity (m/s^2).
$\theta_{\rm CS}$	Angular displacement of the flywheel (rad).
θ_i	Angular displacement of the turbine (rad).
θ_t	Angular displacement of transmission (rad).
θ_p	Angular displacement of the propeller shaft (rad).
ρ	Average density of the vehicle material (kg/m^3).
$\tau_{\rm brake}$	Brake torque (N·m).
B	Damping coefficient of transmission (kg/s).
$R_{\rm dcm}$	DC motor armature resistance (Ω).
K_τ	DC motor torque coefficient (constant).
K_B	DC motor back-EMF coefficient (constant).
I	DC motor current (A).
$L_{\rm dcm}$	DC motor armature inductance (H).
θ	DC motor angular displacement (rad).
C_D	Drag coefficient (constant).
τ_w	Drive shaft output torque (N·m).
J_e	Flywheel moment of inertia (kg·m^2).
i_t	Gear ratio (ratio).
τ_i	Impeller torque (N·m).
U	Longitudinal speed of the vehicle (m/s).
τ_d	Output torque produced by the final drive (N·m).
θ_f	Output angular displacement of the final drive (rad).
θ_w	Output angular displacement of the drive shaft (rad).
A_f	Projected front area of the vehicle (m^2).
τ_p	Propeller shaft input torque (N·m).
τ_f	Propeller shaft output torque (N·m).
$V_{\rm PWM}$	PWM voltage signal applied to the dc motor (V).
$C_{\rm rr}$	Rolling resistance coefficient (constant).
$\theta_{\rm road}$	Road gradient (rad).
K	Stiffness of transmission (kg/s^2).
R	Tire radius (m).
$K_{\rm fc}$	Torque converter capacity factor (kg$^{-0.5}$m^{-1}).
$T_{\rm ratio}$	Torque converter torque ratio (ratio).
$N_{\rm ratio}$	Torque converter speed ratio (ratio).
τ_t	Torque output of the torque converter (N·m).
τ_m	Torque produced by the dc motor (N·m).
τ_e	Torque produced by the engine (N·m).
I_t	Transmission inertia (kg·m^2).
τ_t	Turbine torque (N·m).
m	Vehicle mass (kg).
l	Vehicle track length (m).
J_w	Wheel inertia (kg·m^2).

Manuscript received September 8, 2007; revised December 20, 2007. Recommended by Guest Editors F. Karray and C.W. de Silva. This work was supported in part by the Crosby Award at the University of Michigan and in part by National Science Foundation (NSF) CAREER Award CNS-0642719.

R. Verma and D. Del Vecchio are with the Department of Electrical Engineering and Computer Science, University of Michigan, Ann Arbor, MI 48109 USA (e-mail: rajverma@umich.edu; ddv@eecs.umich.edu).

H. K. Fathy is with the Department of Mechanical Engineering, University of Michigan, Ann Arbor, MI 48109 USA (e-mail: hfathy@umich.edu).

Color versions of one or more of the figures in this paper are available online at http://ieeexplore.ieee.org.

Digital Object Identifier 10.1109/TMECH.2008.915820

I. INTRODUCTION

THIS PAPER examines the problem of building a laboratory-scale vehicle whose longitudinal dynamics are similar to those of a full-size high-mobility multipurpose wheeled vehicle (HMMWV). This laboratory-scale vehicle uses hardware-in-the-loop (HIL) simulation, in the sense of matching key dynamics of the full-size HMMWV (e.g., its inertia) physically, while using an onboard processor to simulate the rest. This is performed with the ultimate goal of developing a scaled experimental testbed. This testbed will be used to validate decision and control algorithms for intelligent transportation systems (ITS) applications.

ITS include a wide range of systems from the basic cruise control system, to the more advanced adaptive cruise control system, to more complex systems that exploit embedded wireless communication technology. These systems include cooperative intersection collision avoidance systems, lateral collision avoidance systems, and longitudinal collision avoidance systems [2], [17]. In response to the highway incident statistics [24], several major automotive companies have established research programs focusing on cooperative safety systems [20]. These systems are conceived with three different levels of automation: advise or warn the driver, partially control the vehicle, and fully control the vehicle in emergency situations. Testing autonomous or partly autonomous algorithms directly on a full-scale transportation system is challenging due to cost limitations

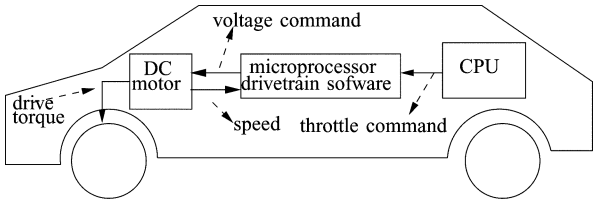

Fig. 1. HIL setup. The hardware of the vehicle includes chassis, wheels, axis, and a dc motor with encoder. The scaled drivetrain dynamics is implemented on the microprocessor controlling the dc motor.

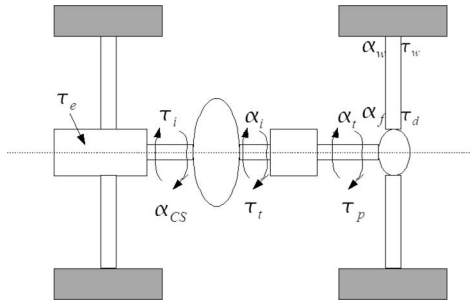

Fig. 2. Drivetrain.

and safety constraints. We are thus developing a lab-scale testbed composed of 1/13-scale vehicles to validate decision and control algorithms for cooperative intersection collision avoidance systems. In such a testbed, the vehicles are equipped with wireless communication, with a positioning system emulating the global positioning system (GPS), and with an on-board computer solving decision, control, and communication tasks. The vehicles' longitudinal dynamics play a central role in collision avoidance algorithms. For a meaningful algorithm validation, it is therefore crucial to design scaled vehicles whose dynamics are a faithful reproduction of the longitudinal dynamics of a full-scale vehicle.

Our scaled vehicle hardware is composed only of the chassis including wheels, tires, axis, and a dc motor with encoder. The unavailability of an exact scaled replica of engine or transmission makes it impossible to include a scaled physical drivetrain on the prototype. Therefore, an HIL setup is designed in which a microprocessor controlling the dc motor emulates the scaled drivetrain dynamics of an HMMWV including engine and transmission. The software coded in the microprocessor takes as input the throttle command by the onboard computer and applies voltage commands to the dc motor in order to obtain the desired drive torque at the wheels. The net result of such an HIL setup is that the system composed of the software on the microprocessor and the dc motor takes as input a throttle command and applies to the wheels the desired drive torque. This way, we are able to obtain a scaled vehicle that as a whole responds to throttle commands in a way similar to the full-scale vehicle. In this paper, we focus on the development and validation of the HIL setup, as shown in Fig. 1. In particular, scaling of the drivetrain dynamics is performed by applying well-known concepts from scaling theory, including the Buckingham π theorem and π groups. Scaling of active components such as engine and transmission is difficult to achieve in hardware. Thus, we come up with an HIL setup and the scaling of these components is carried out in software.

Researchers have been studying scaled vehicles since 1930's for different reasons, such as trailer sway [11], vehicle dynamics [1], [33], performance on rough terrain, and to determine vehicle turning radius [1], for automobile accident reconstruction [12]. More recently, work has been reported on vehicle dynamics and controls [3]–[7], [10], [22], [29], to study the the lateral motion and design of steerimg controller [9], [16], [18], control prototying of braking system (ABS) [21], [23], [25], [26], and to study vehicle rollover [30], [32]. The work that exists in the literature has focused mostly on lateral dynamics. The unique contribution of this paper is the demonstration of longitudinal dynamics scaling of a vehicle with all the active powertrain subsystems present in it using the HIL approach. In making this contribution, we build on well-established HMMWV powertrain and vehicle dynamics models, scaling techniques, and HIL simulation techniques to create a unique scaled testbed for ITS applications. Our validation experiments confirm that the longitudinal response of the scaled vehicle matches the longitudinal response of a full-scale vehicle.

Similitude research has been used for over a century to study the behavior of systems that are difficult to analyze in their original size and normal operating environment. Typically, such research uses scaled models that are dynamically similar to a system much larger than the model. A historic account of development of similitude theory can be found in [7]. Many published studies on this topic are available [6], [7], [27], [28]. Using similitude theory, the dynamics of a system can be studied in terms of dimensionless parameters. An important contributor in the development of this theory is Buckingham [8]. He formulated a theorem, called the π theorem, that can be used to study the scaling properties of any system. See the Appendix for more details.

This paper is organized as follows. In Section II, we describe the drivetrain model that we consider. In Section III, we perform the computation of the π groups and simulate the scaled model to show the match with the full-scale model. In Section IV, we implement the scaled dynamics on the microprocessor. In Section V, we show experimental results and validate the obtained data against the simulation data of the scaled model.

II. Drivetrain Model

The literature presents physics-based models of the longitudinal and powertrain dynamics of the HMMWV, as well as explanations of the assumptions underlying these models [13]–[15], [19]. This paper adopts these models, as described briefly next. Fig. 2 shows the schematic of a vehicle drivetrain. We consider a 4-speed vehicle with automatic transmission and rear wheel drive.

A. Engine

The engine produces torque resulting from the combustion process. The engine is modeled as a map (Fig. 3 [13]), which takes throttle command and engine speed as input and calculates torque generated by the engine, τ_e. For the low-frequency

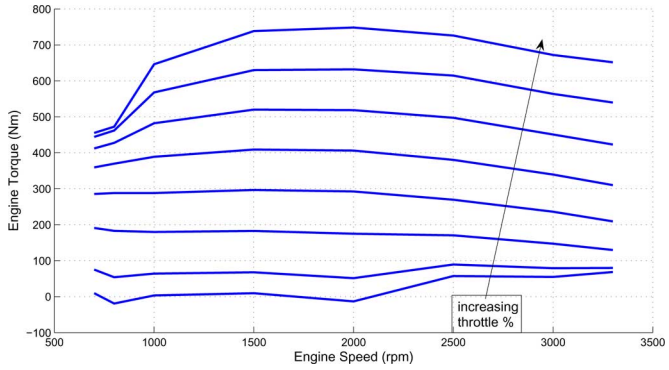

Fig. 3. Engine map [13].

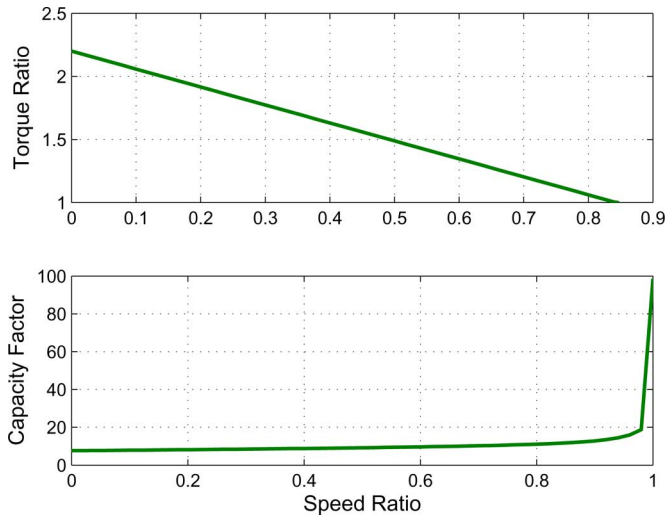

Fig. 4. Torque converter characteristics [13].

dynamics that we are interested in, a map-based engine model can be used. Engine acceleration is calculated from (1), which takes as input engine torque, τ_e, and load torque from torque converter, τ_i. The flywheel is modeled as inertia. The governing equation for the engine and flywheel is

$$J_e \ddot{\theta}_{\rm CS} = \tau_e - \tau_i \tag{1}$$

where J_e is the engine and flywheel moment of inertia, $\ddot{\theta}_{\rm CS}$ is the acceleration of the flywheel, τ_e is the torque produced by the engine, and τ_i is the impeller torque.

B. Torque Converter

The torque converter model is a tabular relationship between the impeller torque, τ_i, the turbine torque, τ_t, the impeller speed, which is assumed to be equal to $\dot{\theta_{\rm CS}}$, and the turbine speed, $\dot{\theta}_i$. The inputs to this model are speed ratio, $N_{\rm ratio} = \dot{\theta}_i / \dot{\theta_{\rm CS}}$, and impeller speed. The capacity factor, $K_{\rm fc}$, and the torque ratio, $T_{\rm ratio}$, are determined by the map shown in Fig. 4. The impeller torque and turbine torque are calculated as

$$\tau_i = \frac{\dot{\theta_{\rm CS}}^2}{{K_{\rm fc}}^2} \tag{2}$$

$$\tau_t = T_{\rm ratio} \tau_i. \tag{3}$$

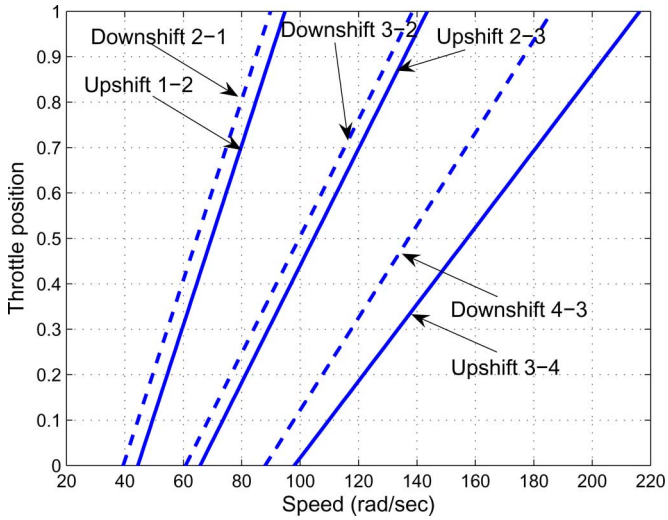

Fig. 5. Shiftmap (taken from [13]).

C. Transmission

The transmission is modeled as a variable gear ratio transformer. To derive transmission dynamics, we treat it as a mass–spring–damper system. This system takes as input the torque output of the torque converter, τ_t, and the gear ratio, i_t. It produces propeller shaft input torque, τ_p. The model is given by

$$\begin{bmatrix} I_t \ddot{\theta}_i \\ \dot{\theta}_i - \dot{\theta}_t i_t \end{bmatrix} = \begin{bmatrix} \frac{-B}{I_t} & -K \\ \frac{1}{I_t} & 0 \end{bmatrix} \begin{bmatrix} I_t \dot{\theta}_i \\ \theta_i - \theta_t i_t \end{bmatrix} + \begin{bmatrix} 1 & B \\ 0 & -1 \end{bmatrix} \begin{bmatrix} \tau_t \\ \dot{\theta}_t i_t \end{bmatrix} \tag{4}$$

$$\tau_p = \begin{bmatrix} \frac{B}{I_t} & K \end{bmatrix} \begin{bmatrix} I_t \dot{\theta}_i \\ \theta_i - \theta_t i_t \end{bmatrix} \begin{bmatrix} 0 & B \end{bmatrix} \begin{bmatrix} \tau_t \\ \dot{\theta}_t i_t \end{bmatrix} \tag{5}$$

in which B is the damping coefficient, I_t is the inertia, and K is the stiffness of the transmission.

D. Shift Logic

Gear shift is modeled as a shift map (Fig. 5), which takes propeller shaft speed and throttle position commanded by the driver as the input and determines the instantaneous gear ratio as the output [13]. Torque and speed variations during the gear shift are captured by incorporating a blending function into the model. The blending function (Fig. 6) gives the variation of torque ratio and speed ratio during the gearshift and captures important dynamics observed during a gearshift [13], [19].

E. Propeller Shaft

The propeller shaft dynamics are taken into account in the transmission model, and thus, the propeller shaft input torque, τ_p, and speed, $\dot{\theta}_t$, are equal to the output torque, τ_f, and speed, $\dot{\theta}_p$

$$\tau_f = \tau_p \tag{6}$$

$$\dot{\theta}_t = \dot{\theta}_p. \tag{7}$$

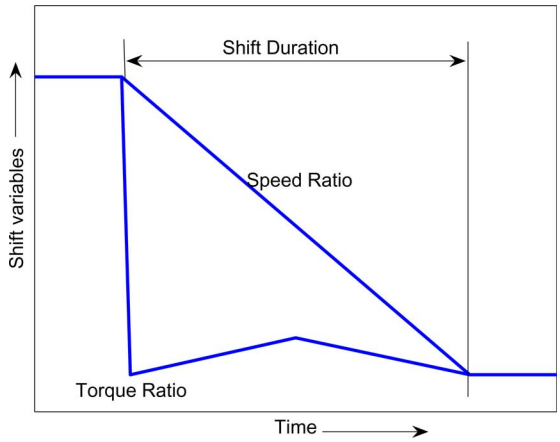

Fig. 6. Blending function (taken from [13]).

F. Final Drive

The final drive is modeled as a ratio, i_f, which reduces the input speed, $\dot{\theta}_p$, and increases the input torque, τ_f, to produce the output speed, $\dot{\theta}_f$, and torque, τ_d, respectively

$$\tau_d = \tau_f i_f \tag{8}$$

$$\theta_p = \theta_f i_f. \tag{9}$$

G. Drive Shaft

The drive shaft dynamics are taken into account in the transmission model, and thus, the drive shaft input torque, τ_d, and speed, $\dot{\theta}_f$, are equal to the output torque, τ_w, and speed, $\dot{\theta}_w$:

$$\tau_w = \tau_d \tag{10}$$

$$\dot{\theta}_w = \dot{\theta}_f. \tag{11}$$

H. Vehicle Model

Point mass vehicle model is considered here, in which we consider only longitudinal vehicle dynamics. We do not address the lateral vehicle dynamics in this paper. This will be addressed in a separate paper. The longitudinal motion of the vehicle is defined by

$$(J_w + mR^2)\ddot{\theta}_w = \tau_w - \tau_{\text{brake}} - \frac{\rho_{\text{air}}}{2} C_D A_f U^2 R - C_{\text{rr}} mg - Rmg\sin(\theta_{\text{road}}) \tag{12}$$

where J_w is the wheel inertia, m is the mass of the vehicle, τ_{brake} is the brake torque, U is the longitudinal vehicle velocity, ρ_{air} is the air density, C_D is the drag coefficient, A_f is the projected front area of the vehicle, C_{rr} is the rolling resistance cofficient, R is the tire radius, and θ_{road} is the road gradient, assumed 0 here.

The system, (1)–(12), is simulated using the Simulink. The main components modeled are engine, automatic transmission, gear shift logic, shafts, and vehicle. This constitutes a point mass longitudinal dynamics model that does not account for roll and pitch. The model considered serves well the purpose of predicting the behavior of an HMMWV in longitudinal maneuvers in the frequency range relevant for control (including the lowest resonance modes of the driveline), and is simple enough to be programmable on the motion controller, given its processing and memory constraints.

TABLE I
PARAMETERS AND VARIABLES ASSOCIATED WITH THE VEHICLE

Engine	$Throttle, J_e, \theta_{CS}, \tau_e, \tau_i$
Torque Converter	$\tau_t, K_{fc}, T_{ratio}, N_{ratio}$
Transmission	$\theta_i, \theta_t, I_t, \tau_p, i_t, B, K$
Propeller shaft, Final drive and Drive shaft	$\theta_p, \theta_f, \theta_w, \tau_f, \tau_d, \tau_w, i_f$
Vehicle model	$Brake, R, m, \tau_{brake}, \tau_w$ $U, l, J_w, \rho_{air}, C_D, A_f, C_{rr}$

TABLE II
PARAMETERS ASSOCIATED WITH THE VEHICLE IN TERMS OF FUNDAMENTAL QUANTITIES

$N_{ratio}, T_{ratio}, i_t, i_f$	$ratio$	$[M^0L^0T^0]$
$\theta_{CS}, \theta_i, \theta_t, \theta_p, \theta_f, \theta_w$	$radians$	$[M^0L^0T^0]$
$Throttle, Brake$	$percentage$	$[M^0L^0T^0]$
$\tau_e, \tau_i, \tau_t, \tau_p, \tau_f, \tau_d, \tau_w$ τ_{brake}	Nm	$[M^1L^2T^{-2}]$
J_e, I_t, J_w	kgm^2	$[M^1L^2T^0]$
m	kg	$[M^1L^0T^0]$
R, l	m	$[M^0L^1T^0]$
U	m/s	$[M^1L^0T^{-1}]$
ρ, ρ_{air}	kgm^{-3}	$[M^1L^{-3}T^0]$
K_{fc}	$kg^{-0.5}s/m$	$[M^{-0.5}L^{-1}T^1]$
A_f	m^2	$[M^0L^2T^0]$
B	kg^1/s	$[M^1L^0T^{-1}]$
C_D, C_{rr}	$dimensionless$	$[M^0L^0T^0]$

III. SCALING

To apply Buckingham's π theorem to the system described in (1)–(12), the governing dynamical equations are examined. The parameters and variables associated with the system, which are used in this study, are listed in Table I.

The fundamental quantities (basic units) chosen for the formulation of nondimensional groups (π groups) are M, T, and L. Similitude is achieved by grouping the parameters into $(n-m)$ independent nondimensional groups, where n is the number of parameters and m is the number of fundamental quantities. The parameters listed in Table I, which are important to design the scaled vehicle, can be written in terms of fundamental quantities, as illustrated in Table II.

All of the unitless parameters, such as angles and percentages form their own π group. Now, we have three fundamental dimensions and 34 parameters (Table II). Out of these, if we choose m, U, and l as repeating parameters (parameters that can appear in some or all of the π groups), the remaining parameters will form 31 dimensionless π groups.

A list of all the π groups is given in Table III.

A. Design of the Scaled Vehicle

It follows from Buckingham's π theorem that if two dynamical systems are described by the same differential equations, then the solution to these differential equations will be

TABLE III
π GROUPS ASSOCIATED WITH THE SYSTEM

$\pi_1 = Throttle, \pi_2 = Brake$	Non-dimensional driver inputs
$\pi_3 = i_t, \pi_4 = i_f, \pi_5 = N_{ratio}, \pi_6 = T_{ratio}$	Non-dimensional transmission and final drive gear ratio
$\pi_7 = \frac{J_e}{mL^2}, \pi_8 = \frac{J_t}{mL^2}, \pi_9 = \frac{J_w}{mL^2}$	Non-dimensional engine, transmission and wheel inertia
$\pi_{10} = \theta_{CS}, \pi_{11} = \theta_i, \pi_{12} = \theta_t, \pi_{13} = \theta_p, \pi_{14} = \theta_f, \pi_{15} = \theta_w$	Non-dimensional angular displacements
$\pi_{16} = \frac{\tau_e}{mU^2}, \pi_{17} = \frac{\tau_i}{mU^2}, \pi_{18} = \frac{\tau_t}{mU^2}, \pi_{19} = \frac{\tau_p}{mU^2}, \pi_{20} = \frac{\tau_f}{mU^2}, \pi_{21} = \frac{\tau_d}{mU^2}, \pi_{22} = \frac{\tau_w}{mU^2}, \pi_{23} = \frac{\tau_{brake}}{mU^2}$	Non-dimensional torques
$\pi_{24} = K_{fc}\sqrt{mU^2}$	Non-dimensional capacity factor
$\pi_{25} = \frac{R}{l}$	Non-dimensional wheel radius
$\pi_{26} = \frac{\rho L^3}{m}, \pi_{27} = \frac{\rho_{air} L^3}{m}$	Non-dimensional vehicle and air density
$\pi_{28} = \frac{A_f}{l^2}$	Non-dimensional projected front area of vehicle
$\pi_{29} = \frac{BU}{ml}$	Non-dimensional damping
$\pi_{30} = C_D, \pi_{31} = C_{rr}$	Non-dimensional drag and rolling resistance coefficient

scale-invariant if the π groups are the same. To design the scaled vehicle, we thus start with analyzing the π groups given in Table III. For the scaled vehicle to be dynamically similar to the actual vehicle, the value of these π groups should be the same for both the systems. Based on this concept, we can derive the parameter values of the scaled vehicle or of the actual vehicle.

1) Calculation of the Parameter Values for the Scaled Vehicle: The track length of the full-scale vehicle and of the scaled vehicle are fixed. The tire size of the scaled vehicle is calculated by equating the π group corresponding to the tire size of the scaled vehicle to the full-size vehicle as follows (Table III, row 5):

$$\left(\frac{R}{l}\right)_{\text{Full}} = \left(\frac{R}{l}\right)_{\text{Scaled}}$$
$$\left(\frac{0.4412}{3.302}\right) = \left(\frac{R}{0.257}\right)$$
$$D_{\text{scaled}} = 0.0343 \text{ m}. \tag{13}$$

The actual tire diameter of the RC car is 0.033 m. This error is compensated by using a feedforward control loop, as discussed in detail in Section IV.

2) Mass of the Full-Scale Vehicle: The mass of the scaled vehicle is 3.15 kg. Using the π groups corresponding to the vehicle density (Table III—row 6), we calculate the mass of the actual vehicle as follows:

$$\left(\frac{\rho l^3}{m}\right)_{\text{Scaled}} = \left(\frac{\rho l^3}{m}\right)_{\text{Actual}}$$
$$(\rho)_{\text{Scaled}} = (\rho)_{\text{Actual}} \text{ (assumed)}$$
$$\left(\frac{l^3}{m}\right)_{\text{Scaled}} = \left(\frac{l^3}{m}\right)_{\text{Actual}}$$
$$\left(\frac{3.302^3}{m}\right)_{\text{Actual}} = \left(\frac{0.257^3}{3.15}\right)_{\text{Scaled}}$$
$$m_{\text{Actual}} = 6681 \text{ kg}. \tag{14}$$

Note that the gross vehicle weight of the full-scale vehicle is 5112 kg [13]. In this paper, it is assumed that the full-scale vehicle is carrying a payload of 1569 kg.

3) Velocity of the Scaled Vehicle: To find the ratio of velocity that the scaled vehicle should maintain with respect to the full-scale vehicle in response to the same input, first observe that time is not being scaled. Thus, we can consider Ut/l to form another π group. Now, we can write

$$\left(\frac{Ut}{l}\right)_{\text{Scaled}} = \left(\frac{Ut}{l}\right)_{\text{Actual}}$$
$$\frac{U_{\text{full}}}{U_{\text{Scale}}} = 3.302/0.257 = 12.84. \tag{15}$$

Thus, the full-scale vehicle velocity should be 12.84 times the velocity of the scaled vehicle when the same maneuver is performed on both the systems.

4) Moment of Inertia of the Scaled Engine: The moment of inertia of the engine in the full-scale HMMWV is 0.5 kg m^2 [14]. We proceed as follows to scale the moment of inertia:

$$\left(\frac{J_e}{ml^2}\right)_{\text{Scaled}} = \left(\frac{J_e}{ml^2}\right)_{\text{Scaled}}$$
$$\left(\frac{J_e}{3.15(0.257^2)}\right)_{\text{Scaled}} = \left(\frac{.5}{6681(3.302^2)}\right)_{\text{Actual}}$$
$$J_{e\text{Scaled}} = 1.51 \times 10^{-6} \tag{16}$$

which gives the moment of inertia of the scaled engine.

5) Engine Torque Scaling: To determine the ratio of torque produced by the engine of the scaled vehicle to the full-scale vehicle, the π groups corresponding to engine torque are equated (Table III—row 2). We thus obtain the following relation:

$$\left(\frac{\tau_e}{mU^2}\right)_{\text{Scaled}} = \left(\frac{\tau_e}{mU^2}\right)_{\text{Actual}}$$
$$(\tau_e)_{\text{Scaled}} = 2.855 * 10^{-6} \, (\tau_e)_{\text{Actual}} \tag{17}$$

This torque scaling is used to scale the engine torque map (Fig. 3).

It is difficult to measure parameters such as I_t, J_w, A_f, B, C_D, and C_{rr} for the scaled vehicle. The difference in these parameters is compensated by simulating it in the HIL setup and will be discussed in Section IV-A.

B. Validation of the Scaled Model

The validation of the derived π groups and scaled vehicle design based on these groups is done in two steps. A simulation of the scaled model is carried out as a first step and is discussed in this section. This is followed by experimental tests with the scaled vehicle hardware. These are discussed in Section V.

This section presents the simulation results of the scaled vehicle compared to the full-scale vehicle. All parameters of the scaled model are derived, as illustrated in Section III-A. The

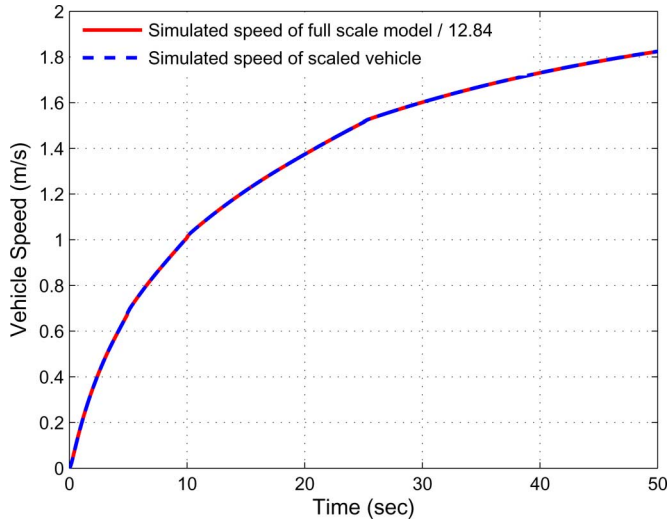

Fig. 7. Scaled vehicle velocity versus full-scale vehicle velocity.

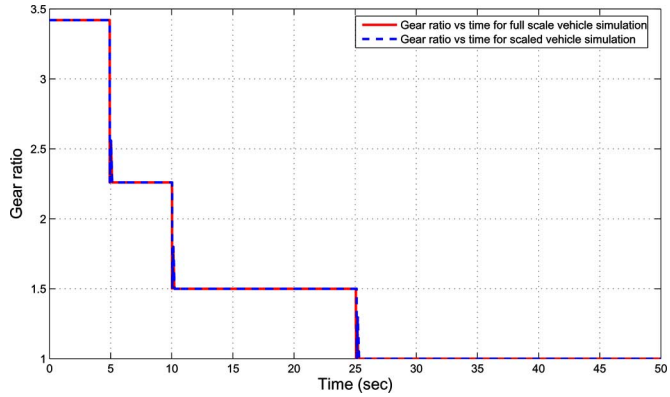

Fig. 8. Scaled vehicle gear ratio versus full-scale vehicle gear ratio.

full-scale and scaled vehicle simulations are carried out for the same input commands. It is found that the longitudinal velocity of the full-scale vehicle is 12.84 times the velocity of the scaled vehicle (Fig. 7). The gearshift in both full scale and scaled vehicles occurs at the same time, as shown in Fig. 8.

IV. Implementation on Scaled RC Car

A Tamiya scaled RC car chassis[1] is used as the hardware platform to implement the scaled dynamics and validate the simulation results. The vehicle originally had four-wheel drive. A quadrature encoder is used to sense the tire speed. The front axle of the vehicle is modified to fit the encoder and it no longer drives the vehicle. Thus, the vehicle has rear wheel drive and front wheel steering.

Fig. 9 shows the system architecture. In the present configuration, a human driver issues throttle, brake, and steer commands through a central control station. These commands are transmitted to the onboard computer (Mini ITX) through a wireless connection. These commands act as input to the driveline dynamics, which are programmed on the motion controller. The

[1][Online]. Available: http://www.tamiyausa.com/

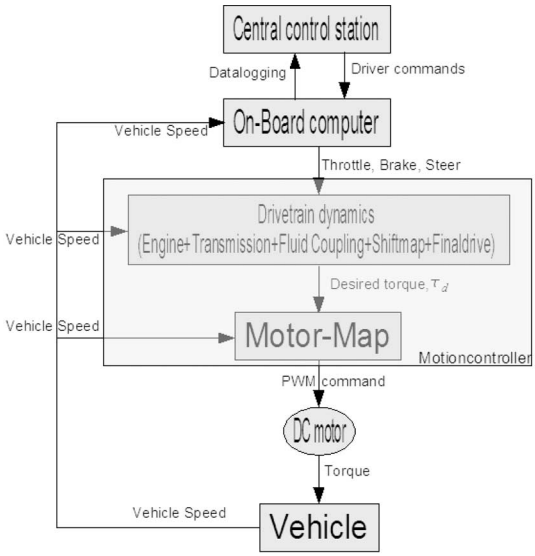

Fig. 9. Scaled vehicle command flow.

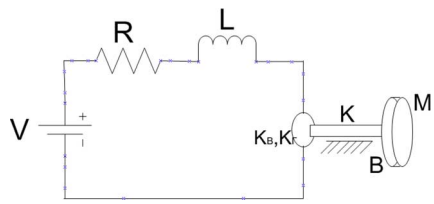

Fig. 10. Electromechanical system.

driveline dynamics consist of the engine, fluid coupling, transmission, and gearshift logic, as explained in Section II. Shift logic is programmed in the form of a shift map. The output of this program is the drive torque, τ_d.

The drive torque is the torque that should be applied to the wheels. Since we have a dc motor, it is difficult to measure or control such a torque because of the absence of current measurement. To overcome this problem, a set of experiments were performed to identify the relationship between drive torque and motor voltage for any given wheel speed. This is discussed in the next section. Vehicle speed is measured using an optical encoder and is used for calculations in drivetrain and motor map blocks. This speed is sent to the onboard computer and is transmitted to the central control station through a wireless connection, where it is recorded.

A. DC Motor System Identification

The dynamics of the electromechanical system (Fig. 10) comprising a car being run by the dc motor includes three parts: 1) A dynamic mechanical subsystem, which is the scaled vehicle; 2) a dynamic electrical subsystem, which includes all of the motor's electrical effects; and 3) a static relationship that represents the conversion of electrical quantities into mechanical torque. Assuming very high torsional stiffness of drivetrain components transmitting torque, the mechanical subsystem dynamics of the vehicle run by a permanent-magnet brush dc motor

are assumed to be of the form

$$M\ddot{\theta} + B\dot{\theta} = \tau_m \tag{18}$$

in which

$$M = J_w + mR^2$$

and

$$\tau_m = K_\tau I.$$

The motor armature current, $I(t)$, is given by the electrical subsystem dynamics for the permanent magnet brush DC motor, which is assumed to be of the form

$$L_{\rm dcm}\dot{I} = V_{\rm PWM} - R_{\rm dcm} I - K_B\dot{\theta} \tag{19}$$

in which, J_w is the wheel moment of inertia, m is the vehicle mass, B is the damping in the drivetrain, K is the stiffness in drivetrain, $\theta(t)$ is the angular motor position, K_τ is the coefficient that characterizes the electromechanical conversion of armature current to torque, $L_{\rm dcm}$ is the armature inductance, $R_{\rm dcm}$ is the armature resistance, K_B is the back-EMF coefficient (which is equal to K_τ), and $V_{\rm PWM}$ is the pulse width modulation voltage signal supplied to the dc motor. For the aforesaid model, the states θ and $\dot{\theta}$ are easy to measure while I is difficult to measure. Because of the inability to measure motor current I, the control of the torque produced by the motor is hard. This difficulty is overcome by noticing that in this mechatronic system, the time constant of the electrical subsystem is faster than the mechanical subsystem. This means that we can assume the current and voltage to be statically related. This allows us to perform system identification of the electromechanical system to obtain $V_{\rm PWM}$ versus speed ($\dot{\theta}$) versus total torque ($\tau_{\rm total}$) map. Assuming $L_{\rm dcm}$ to be negligible, we can write (19) as

$$I = \frac{V_{\rm PWM}}{R_{\rm dcm}} - \frac{K_B\dot{\theta}}{R_{\rm dcm}}. \tag{20}$$

From (18), we have

$$M\ddot{\theta} + \left(B + K_\tau \frac{K_B}{R_{\rm dcm}}\right)\dot{\theta} - K_\tau \frac{V_{\rm PWM}}{R_{\rm dcm}} = 0. \tag{21}$$

$M\ddot{\theta}$ is the torque that accelerates the vehicle. We call it the total torque, $\tau_{\rm total}$. It is equal to the torque produced by the motor minus the torque lost in damping of the scaled vehicle. Our objective is to be able to control the torque generated by the dc motor, τ_m, and make it proportional at all time to the torque generated by the engine, τ_e, that is programmed on the motion-controller. As stated earlier, this is a hard problem in the absence of current measurement. Though τ_m cannot be measured, $\tau_{\rm total}$ can be determined experimentally. We shift the problem from trying to make τ_e proportional to τ_m to making $\tau_d = \tau_{\rm total}$. The torque $\tau_{\rm total}$ corresponds to the torque generated by the drivetrain that accelerates the vehicle, i.e., τ_d. In order to solve this problem, we identify the coefficients of $\dot{\theta}$ and of $V_{\rm PWM}$ in (21) by running experiments.

Experiments are performed, in which a constant PWM signal ($V_{\rm PWM}$) is applied to the dc motor and the vehicle response (vehicle velocity vs. time) is recorded (Fig. 11 shows an example). The data is logged at a frequency of 7.7 Hz. Vehicle

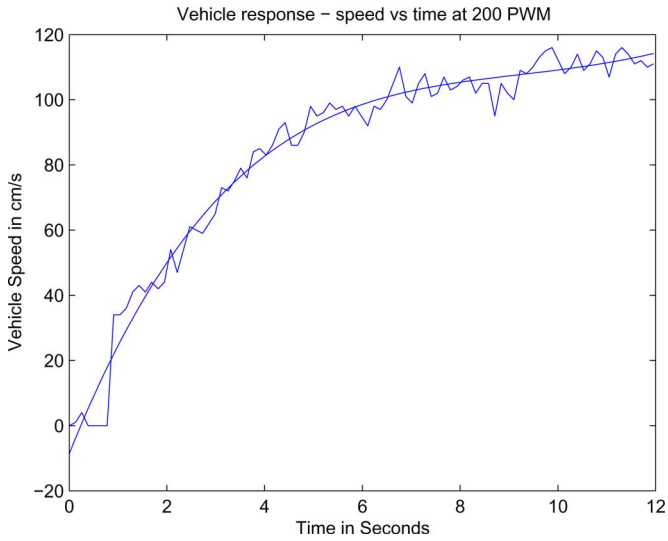

Fig. 11. Vehicle speed versus time.

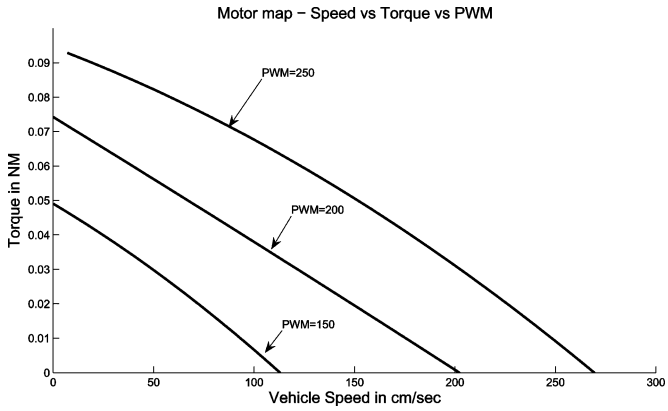

Fig. 12. Motor map.

acceleration is obtained by differentiating the vehicle velocity. As vehicle velocity is noisy, a polynomial fit of the third order to the vehicle velocity versus time curve is used before differentiation to calculate the acceleration a. The value of $\ddot{\theta}$ is calculated from this acceleration as follows:

$$\ddot{\theta}_{\rm wheel} = \frac{a}{R} \tag{22}$$

$$\ddot{\theta} = 7.21\ddot{\theta}_w \tag{23}$$

where, $\ddot{\theta}_w$ is the wheel angular acceleration and 7.21 is the gear ratio of the scaled model. Using (21), $\tau_{\rm total}$ for a given vehicle velocity and PWM signal can be calculated. This data can be plotted as $\tau_{\rm total}$ versus vehicle velocity at a constant PWM. A number of such experiments are performed, for a particular PWM, to check the repeatability of the experiment. PWM signals are chosen to cover the whole range of operation of the dc motor. A motor map is obtained by plotting $\tau_{\rm total}$ versus vehicle velocity at a constant PWM value, as shown in Fig. 12. In calculating M, we consider J_w negligible when compared to mR^2.

To use this map on a running vehicle at any instant of time, the drivetrain block (Fig. 9) calculates the torque that is to be

TABLE IV
BASIC SPECIFICATIONS OF THE SCALED MODEL

Overall length	375mm, Width: 185mm, Wheelbase: 257mm, Weight: 890g
Transmission type	Longitudinally mounted motor with shaft-driven 4WD
Gear ratio	7.21:1
Suspension	Double wishbone (front and rear)
Damper	CVA oil dampers (front and rear
Tire Width	27mm, Diameter: 67mm
Tread Pattern	Racing slick

TABLE V
BASIC SPECIFICATIONS OF THE DC MOTOR.

Turns	25
Voltage	7.2 Volt
Speed	Unloaded RPM 19000
Maximum Torque	500 gf/cm (Gram Force per Centimeter) @ 7.2V

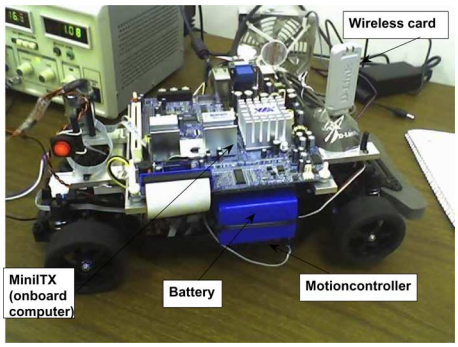

Fig. 13. Scaled vehicle.

applied to the scaled vehicle. The PWM that has to be supplied to the dc motor to generate this torque, given the velocity of the scaled vehicle and required τ_d is given by

$$V_{\mathrm{PWM}} = k_1 \tau_d + k_2 v \tag{24}$$

where v is the vehicle velocity, and k_1 and k_2 are constants that are determined by performing system identification on the motor map. The values calculated were $k_1 = 2503$ and $k_2 = 1$. However, during experimentation, we found that the relation that produced the best response was

$$V_{\mathrm{PWM}} = 70 + 2800\tau_d + 0.72v.$$

The experiments were conducted as a constant throttle performance for 30%, 40%, and 50% throttle. The values of k_1 and k_2 are found to be different for these three cases, though not significantly. The values of k_1 and k_2 are thus kept constant corresponding to 30% throttle for the rest of this paper.

B. Description of the Scaled Vehicle Hardware

In this section, specifications of the scaled vehicle hardware are provided. The scaled vehicle specifications are given in Table IV.

1) Motor Specifications: The model uses GT-tuned-motor (25T), which is a replaceable brush standard-type electric motor. The motor specifications are provided in Table V.

2) Electronic Architecture: Each vehicle (Fig. 13) is equipped with a motion controller (BrainStem module) implementing the scaled driveline dynamics of an HMMWV (Section II). The onboard computer (running Linux, Fedora core) communicates with the motion controller by means of a serial connection. The computer is also equipped with wireless communication capability. The computer handles the high-level control functions by commanding steering, braking, and throttle to the motion controller. The motion controller offers two channels of high-resolution motion control. These channels offer flexible PWM or PID control of motors with various types of feedback including encoders, quadrature encoders, analog input, and back-EMF speed control. The motion controller can handle a variety of motion control needs. This processor can run concurrent tiny embedded application (TEA) programs, reflexes, and handle slave commands from a host personal computer (PC), all simultaneously. The motion controller board can accept two 3 Amp H-Bridge with back-EMF control. Access to the module is through a console application and C language.[2]

C. Description of the Scaled Vehicle Software

The high-level control algorithms are programmed on the onboard computer. A datalogging module is programmed on the onboard computer, which can read vehicle speed from the motion controller at a frequency of 10 samples/s. The drivetrain components, including engine, fluid coupling, transmission, gear shift logic, and final drive are programmed on the motion controller. The motion controller issues control signals to the steering servo and controls the PWM signal to the dc motor. The programming on the motion controller is performed in the TEA language, described in the next section.

1) Brainstem TEA Language: The TEA[3] language is a subset of the C programming language. TEA has integer math operations, simple looping constructs, conditional statements, and parameterized subroutines. It is ideally suited for simple control loops, sequencing behaviors in robotics, and other tasks that can be offloaded from the main controller of a complex system. TEA is precompiled, enabling conditional compilation, macros, and inclusion of other files. Programs are typically very small and have no memory allocation, structures, or objects. All variables are stack based; the stack can be very small in some environments, so minimal recursion is possible. Program compilation is done through the console application. The compiler translates the TEA language file into the virtual machine's specific instructions (opcodes).

V. EXPERIMENTS

A number of experiments were performed to ascertain the behavior of the scaled vehicle and its dynamic similitude to an HMMWV. The following sections discuss the experimental setup and results.

[2][Online]. Available: www.acroname.com/brainstem/tea/tea1.html
[3][Online]. Available: www.acroname.com/robotics/parts/s10-moto-brd.html

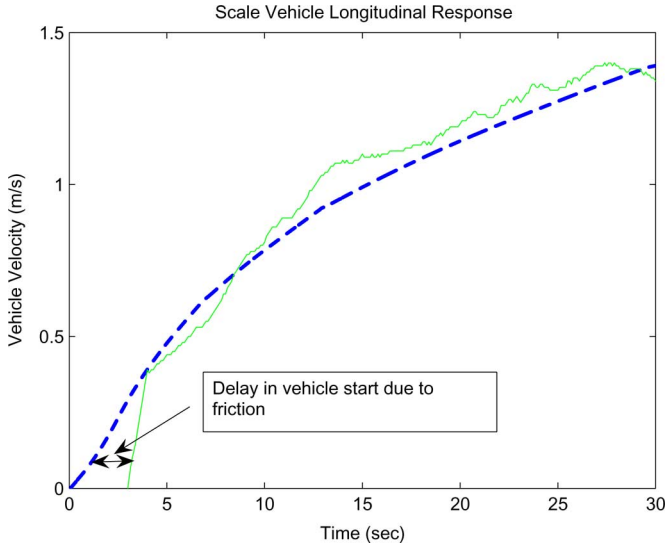

Fig. 14. Scale vehicle speed versus time for 40% throttle.

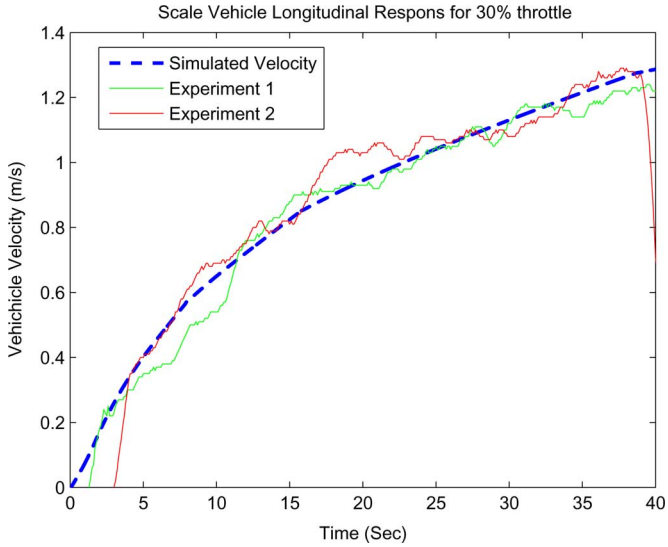

Fig. 15. Vehicle speed versus time for scaled vehicle model and scaled vehicle simulation.

A. Experimental Setup

The scaled vehicle can take throttle, steering, and braking commands from the human driver at a central control station. The driving maneuver that is considered for verifying the longitudinal response of the scaled vehicle vis a vis an actual vehicle is the constant throttle performance test. In this test, a constant throttle input is given to the scaled vehicle and the resulting velocity and gear shift response are logged. This test is repeated for several throttle values (30%, 40%, 50%). The fourth-floor corridor in the electrical engineering and computer science building is utilized for testing because the testbed dimension (6.6 m $\times$ 5.6 m) is not sufficient to run the vehicle for significant length and duration. All communication to and from the scaled vehicle is through a local wireless network from the laboratory. The maximum length that is avialable with wireless coverage is limited to 42.67 m. This also restricts the length of a test run.

Throttle inputs more than 50% cannot be applied because of the difficulty in controlling the vehicle at high speed while conducting the experiment in the corridor. During the experiments, the voltage supply to the scaled vehicle has to be kept constant at 15.4 V. Therefore, for this test, we power the vehicle through a power supply method instead of using the onboard batteries. One person carrying the power supply has to follow the vehicle while it is running. Due to the limited length of the corridor, the steady state speed of the vehicle is never achieved. This issue is not relevant for this research because it is not expected to experience high speed of the scaled vehicle in the testbed, which is only 6.6 $\times$ 5.6 m. Since the purpose of this testbed is to test algorithms for multiagent traffic intersection, we do not expect to attain high velocities or steady state response of the vehicle.

It is observed during the experiments that the scaled vehicle does not start as soon as the throttle command is applied by the driver. There is a delay between the application of throttle command and start of the vehicle. An external excitation is required to set the vehicle into motion. This can be attributed to the friction in the scaled hardware drivetrain.

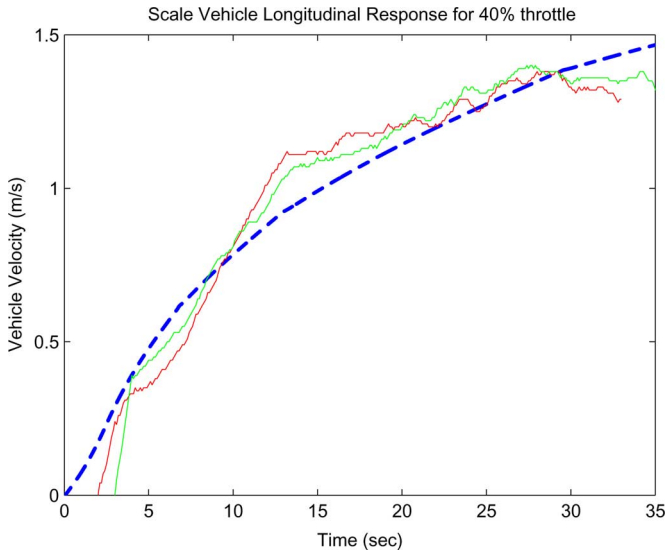

Fig. 16. Vehicle speed versus time for scaled vehicle model and scaled vehicle simulation.

B. Experimental Results

Fig. 14 shows the speed response of the scaled vehicle vis-a-vis simulation. The delay in start of the vehicle can be clearly seen in Fig. 14.

The results are presented for a constant input of 30%, 40%, and 50% throttle to the vehicle. Figs. 15–17 show the speed response of the scaled vehicle vis-a-vis simulation. It is seen that the response of the scaled vehicle closely follows the simulated response. The average root-mean-square (RMS) error in speed for 30% throttle is 0.0525 m/s, 40% throttle is 0.0809 m/s and 50% throttle is 0.1099 m/s. There seems to be an increasing trend in the RMS error. This, in part, can be attributed to the higher speeds attained by the vehicle with increasing throttle because of which we normalize the RMS error with maximum speed. Normalized RMS error attained by the vehicle with 30%, 40%,

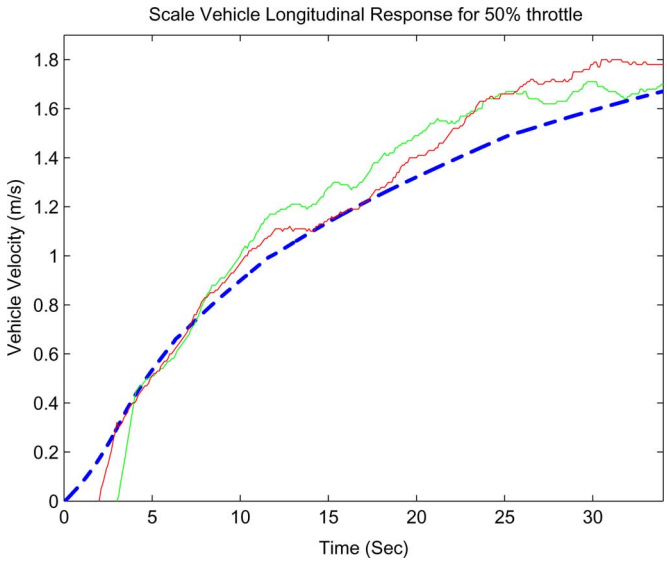

Fig. 17. Vehicle speed versus time for scaled vehicle model and scaled vehicle simulation.

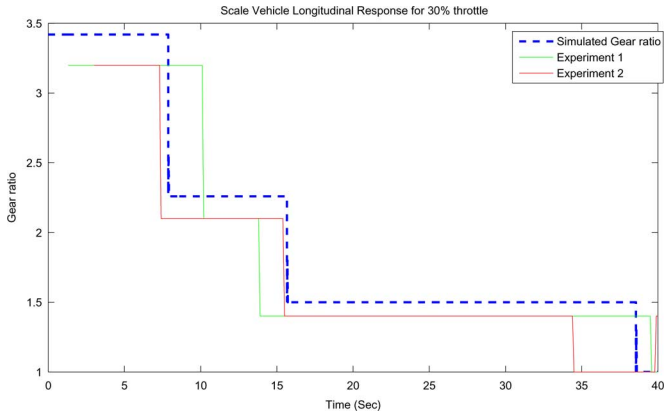

Fig. 18. Gear ratio versus time for scaled vehicle model and scaled vehicle simulation.

and 50% is 0.4375, 0.559, and 0.605, respectively. The lower error for the 30% throttle can be attributed to the fact that the motor map parameters were chosen so as to obtain the best results for the 30% throttle (as explained in Section IV-A).

The gear ratio of the scaled vehicle as compared to the simulation is shown in Figs. 18–20. We see that the gearshift occurs before it is expected to occur, as indicated by the simulation, if the actual speed is more than the simulated speed. Similarly, the gearshift occurs after it is expected to occur, as indicated by the simulation, if the actual speed is less than the simulated speed. This agrees with the observed data. Table VI presents the error in longitudinal response of the prototype versus the scaled vehicle simulation.

Overall, it is observed that the scaled vehicle response matches the simulated response of the scaled vehicle both in terms of speed as well as gear shift versus time. The scaled vehicle simulation was shown to be dynamically similar to an HMMWV in Section III-B. Thus, the match of the experimental vehicle longitudinal response to that of the simulated vehicle is

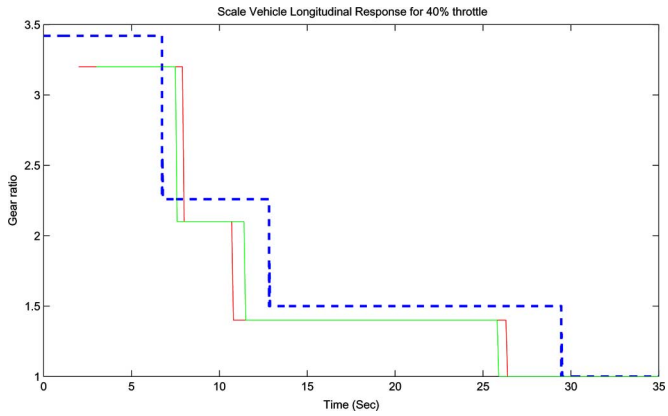

Fig. 19. Gear ratio versus time for scaled vehicle model and scaled vehicle simulation.

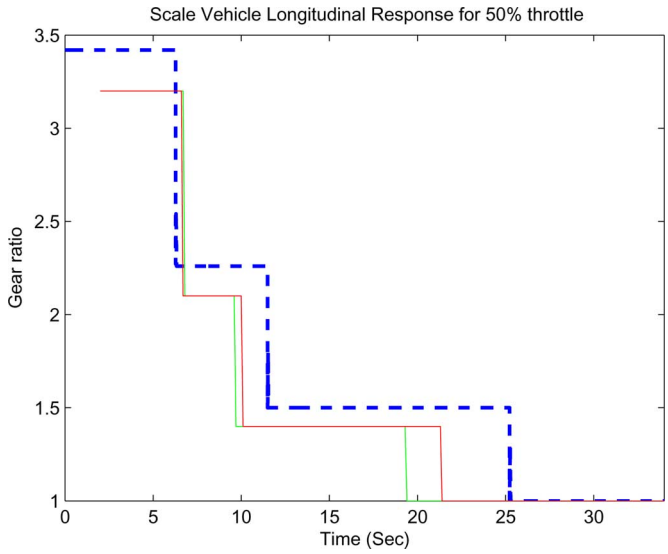

Fig. 20. Gear ratio versus time for scaled vehicle model and scaled vehicle simulation.

TABLE VI
ERROR IN EXPERIMENTAL RESULTS

RMS error in speed for 30 % throttle	0.0525m/s
RMS error in speed for 40 % throttle	0.0809m/s
RMS error in speed for 50 % throttle	0.1099m/s
1st to 2nd gearshift time difference for 30 % throttle	1.25 sec
2nd to 3rd gearshift time difference for 30 % throttle	1 sec
3rd to 4th gearshift time difference for 30 % throttle	2.5 sec
1st to 2nd gearshift time difference for 40 % throttle	1 sec
2nd to 3rd gearshift time difference for 40 % throttle	1.8 sec
3rd to 4th gearshift time difference for 40 % throttle	3.3 sec
1st to 2nd gearshift time difference for 50 % throttle	.45 sec
2nd to 3rd gearshift time difference for 50 % throttle	1.6 sec
3rd to 4th gearshift time difference for 50 % throttle	4.5 sec

sufficient to prove dynamic similitude of the scaled vehicle to an HMMWV.

VI. CONCLUSION

The development of a scaled vehicle that is dynamically similar to an HMMWV has been presented. Models of various subsystems of the full-scale vehicle were introduced and the

scaled vehicle design was carried out. Implementation on a scaled RC car was performed. Experiments demonstrated the dynamic similitude of the scaled vehicle to full-scale vehicle.

APPENDIX

Theorem 1 (F. M. White, Fluid Mechanics, Section 5.3): (Buckingham π Theorem) If a physical process satisfies the principal of dimensional homogeneity and involves n dimensional variables, it can be reduced to a relation between only k dimensionless variables or π's. The reduction $j = n - k$ equals the maximum number of variables that do not form a pi among themselves and is always less than or equal to the number of dimensions describing the variables.

Let $q_1, q_2, \ldots q_n$ be n dimensional variables that are physically relevant in a given problem and that are interrelated by an (unknown or known) dimensionally homogeneous set of equations. These can be expressed via a functional relationship of the form

$$F(q_1, q_2, \ldots q_n) = 0.$$

If k is the number of fundamental quantities required to describe the n variables, then there will be k primary variables and the remaining $j = (n - k)$ variables can be expressed as $(n - k)$ dimensionless and independent quantities or "Pi groups," $\pi_1, \pi_2, \ldots \pi_{n-k}$. The functional relationship can thus be reduced to the much more compact form

$$\Phi(\pi_1, \pi_2, \ldots \pi_{n-k}) = 0.$$

Note that this set of nondimensional parameters is not unique. The π groups are, however, independent [31]. Here, independence means that one π group can be varied while keeping other groups constant. The fundamental quantities of a system consist of the minimum number of unit dimensions needed to describe each parameter. For example, the units of measure for acceleration are length unit/(time unit)^2. The fundamental quantities most often used are mass, length, time, temperature, current, amount of substance, and luminous intensity. Two differently sized physical systems, with different dimensional parameters, can be reduced to the same dimensionless description if the corresponding π parameters have the same numerical values. An example with application of π theorem is given in the next section.

A. An Example: The Simple Pendulum

Consider a simple pendulum, which is a mass m on the end of a massless rod of length l. We wish to investigate what quantities may affect the period τ of this pendulum. In addition to the mass and length of the pendulum, the acceleration due to gravity g, the initial angle θ_0, and the tension in the rod T may have an effect on the period. We ignore elasticity in the rod for this simple example. Thus, we have

$$\tau = F(m, l, g, \theta_0).$$

The next step is to identify for each quantity its dimensions in terms of the fundamental dimensions appropriate for the problem. Each quantity Z will have its dimensions, $[Z]$, written as a product of powers of the fundamental dimensions, $L_1, L_2, \ldots, L_k$

$$[Z] = {L_1}^{\theta_1} {L_2}^{\theta_2} \ldots {L_k}^{\theta_k}.$$

In the case of the simple pendulum, the fundamental dimensions are length $L_1 = L$, mass $L_2 = M$, and time $L_3 = T$. In terms of these fundamental dimensions, each quantity has the following dimensions:

$$[\tau] = [M^0 L^0 T^1], [m] = [M^1 L^0 T^0], [l] = [M^0 L^1 T^0]$$
$$[g] = [M^0 L^1 T^{-2}], [\theta_0] = [M^0 L^0 T^0].$$

The number of fundamental quantities is three, $n = 5$ and $m = 3$. Thus, we have three fundamental quantities and two dimensionless, independent π groups. The angle θ_0 is a dimensionless quantity and its dimension can be denoted by 1. The first π group is $\pi_1 = \theta_0$. π groups are not unique. Different π groups can result based on the selection of repeating variables. Repeating variables appear in more than one π group. Let us consider $m, l,$ and g as the repeating variables

$$[\tau][m^a][l^b][g^c] = [MLT]^0.$$

This means that

$$[T]^1 [M]^a [L]^b ([L][T]^{-2})^c = [MLT]^0.$$

The dimensions of T, L, and M should match on both sides of this relationship. Equating exponents on both sides leads to the following set of linear equations in the three unknowns a, b, and c:

$$a = 0$$
$$b + c = 0$$
$$2c = 1.$$

Solving the aforesaid linear equations, we obtain $a = 0$, $b = -1/2$, and $c = 1/2$. Thus, the second π group is given by, $\pi_2 = \tau\sqrt{g/l}$. The functional relationship of this system can be reduced to the form

$$\Phi(\pi_1, \pi_2) = 0.$$

REFERENCES

[1] M.G. Bekker, *Introduction to TerrainVehicle Systems*. Ann Arbor, MI: Univ. of Michigan Press, 1969.

[2] R. Bishop, *Intelligent Vehicle Technology and Trends*. Norwood, MA: Artech House, 2005.

[3] S. Brennan and A. Alleyne, "A scaled testbed for vehicle control: The IRS," in *Proc. 1999 IEEE Int. Conf. Control Appl.*, pp. 327–332.

[4] S. Brennan and A. Alleyne, "Driver assisted yaw rate control," in *Proc. Amer. Controls Conf.*, San Diego, CA, 1999, pp. 1697–1704.

[5] S. Brennan and A. Alleyne, "The Illinois roadway simulator: A mechatronic testbed for vehicle dynamics and control," *IEEE/ASME Trans. Mechatronics*, vol. 5, no. 4, pp. 349–359, Dec. 2000.

[6] S. N. Brennan, "Modeling and control issues associated with scaled vehicles," Master's thesis, Univ. Illinois at Urbana Champaign, Urbana Champaign, 1999.

[7] S. N. Brennan, "On size and control: The use of dimensional analysis in controller design," Ph.D. thesis, Univ. Illinois at Urbana Champaign, Urbana Champaign, 2002.

[8] E. Buckingham, "On physically similar systems: Illustration of the use of dimensional equations," *Phys. Rev.*, vol. 4, pp. 345–376, 1914.

[9] S. R. Burns, R. T. O'Brien Jr., and J. A. Piepmeier, "Steering controller design using scale-model vehicles," in *Proc. 34th Southeastern Symp. Syst. Theory*, 2002, pp. 476–478.
[10] M. DePoorter, S. Brennan, and A. Alleyne, "Driver assisted control strategies: Theory and experiment," in *Proc. 1998 ASME Int. Mech. Eng. Congr. Expo.*, pp. 721–728.
[11] L. Huber and O. Dietz, "Pendelbewegung Von Lastkraftwagen—Anhanger und iher Vereidung," *VDI-Zeitschrift*, vol. 81, no. 16, pp. 459–463, 1937.
[12] R. I. Emori, "Automobile accident reconstruction: UCLA motor vehicle safety contract final report," Univ. California at Los Angeles, Los Angeles, Tech. Rep., 1969.
[13] H. K. Fathy, R. Ahlawat, and J. L. Stein, "Proper powertrain modeling for engine-in-the-loop-simulation," in *Proc. ASME Int. Eng. Congr. Expo., IMECE2005-81592*, 2006, vol. 74, pp. 1195–1201.
[14] Z. S. Filipi, H. Fathy, J. R. Hagena, A. Knafl, R. Ahlawat, J. Liu, D. Jung, D. N. Assanis, H. Peng, and J. Stein, "Engine-in-the-loop testing for evaluating hybrid propulsion concepts and transient emissions—HMMWV case study," presented at the SAE 2006 World Congr. Exhib., Detroit, MI, Apr.
[15] T. D. Gillespie, *Fundamentals of Vehicle Dynamics*. Warrendale, PA: SAE Int., Mar. 1992.
[16] P. Hoblet, R. T. O'Brien, Jr., and J. A. Piepmeier, "Scale-model vehicle analysis for the design of a steering controller," in *Proc. 35th Southeastern Symp. Syst. Theory*, 2003, pp. 201–205.
[17] Intelligent Vehicle Initiative. (2005). Final report [Online]. Available: http://www.itsdocs.fhwa.dot.gov/JPODOCS/REPTS_PR/14153_files/ivi.pdf
[18] R. T. O'Brien, Jr., J. A. Piepmeier, P. C. Hoblet, S. R. Burns, and C. E. George, "Scale-model vehicle analysis using an off-the-shelf scale-model testing apparatus," in *Proc. 2004 Amer. Control Conf.*, Jun., pp. 3387–3392.
[19] U. Kiencke and L. Nielsen, *Automotive Control Systems, For Engine, Driveline, and Vehicle*, 2nd ed. New York: Springer-Verlag, 2005.
[20] K. Laberteaux, L. Caminiti, D. Caveney, and H. Hada, "Pervasive vehicular networks for safety," *IEEE Pervasive Comput., Spotlight*, vol. 5, no. 4, pp. 60–62, Oct. 2006.
[21] R. G. Longoria, A. Al-Sharif, and C. Patil, "Scaled vehicle system dynamics and control: A case study on anti-lock braking," *Int. J. Veh. Auton. Syst.*, vol. 2, no. 1/2, pp. 18–39, 2004.
[22] D. Lynch and A. Alleyne, "Velocity scheduled driver assisted control," *Int. J. Veh. Des.*, vol. 29, pp. 1–22, Aug. 2003.
[23] A. Mathews, "Implementation of a fuzzy rule based algorithm for adaptive antilock braking in a scaled car," Master's thesis, Univ. Texas at Austin, Austin, 2002.
[24] U.S. Department of Transportation Federal Highway Administration. (2007, Jan.). Road safety fact sheet [Online]. Available: http://safety.fhwa.dot.gov/facts/road_factsheet.htm
[25] C. B. Patil, R. G. Longoria, and J. Limroth, "Control prototyping for an anti-lock braking control system on a scaled vehicle," in *Proc. 42nd IEEE Conf. Decis. Control (CDC 2003)*, vol. 5, pp. 4962–4967.
[26] C. Patil, "Anti-lock brake system re-design and control prototyping using a one-fifth scale vehicle experimental test-bed," Master's thesis, Univ. Texas at Austin, Austin, 2003.
[27] M. Polley, "Size effects on steady state pneumatic tire behavior: An experimental study," Master's thesis, Univ. Illinois at Urbana Champaign, Urbana Champaign, 2001.
[28] M. Polley, A. Alleyne, and E. D. Vries, "Scaled vehicle tire characteristics: Dimensionless analysis," *Veh. Syst. Dyn.*, vol. 44, no. 2, pp. 87–105, Feb. 2006.
[29] A. Alleyne, S. Brennan, and M. DePoorter, "The Illinois roadway simulator—A hardware-in-the-loop testbed for vehicle dynamics and control," in *Proc. Amer. Control Conf.*, Philadelphia, PA, 1998, vol. 1, pp. 493–497.
[30] W. E. Travis, R. J. Whitehead, D. M. Bevly, and G. T. Flowers, "Using scaled vehicles to investigate the influence of various properties on rollover propensity," in *Proc. 2004 Amer. Control Conf.*, pp. 3381–3386.
[31] F. M. White, *Fluid Mechanics*. New York: McGraw-Hill, 1989.
[32] R. J. Whitehead, D. M. Bevly, and B. Clark, "ESC effectiveness during property variations on scaled vehicles," presented at the 2005 ASME IMECE, Orlando, FL, vol. 5.
[33] Y. H. Zakin, "Pritchine vozniknovenya pritsepov (The cause of instability of trailers)," *Avtom. Promyshlennost (Russian Automotive Ind. J.)*, vol. 11, 1959.

Rajeev Verma (S'08) received the Bachelor's degree in mechanical engineering in 2003 from the National Institute of Technology, Warangal, India. He is currently working toward the Ph.D. degree at the University of Michigan, Ann Arbor.

From 2003 to 2005, he was with Advanced Engineering, Ashok Leyland, Ltd., India. Since January 2005, he has been a Graduate Student at the University of Michigan. His current research interests include system modeling and control and decision and control in multiagent systems.

Domitilla Del Vecchio received the Laurea degree (*magna cum laude*) in electronic engineering from the University of Rome at Tor Vergata, Rome, Italy, in 1999, and the Ph.D. degree in control and dynamical systems from the California Institute of Technology, Pasadena, in 2005.

In 2006, she joined the Department of Electrical Engineering and Computer Science, University of Michigan, Ann Arbor, where she is currently an Assistant Professor. Her current research interests include the analysis and control of hybrid and embedded systems, with application to multiagent systems such as intelligent transportation and multirobot systems, and the analysis and control of biomolecular systems, with application to synthetic biology.

Dr. Del Vecchio is the recipient of a 2007 National Science Foundation (NSF) CAREER Award.

Hosam K. Fathy was born in 1977. He received the B.Sc. degree (*summa cum laude*) from the American University in Cairo, Cairo, Egypt, in 1997, the M.S. degree from Kansas State University, Manhattan, in 1999, and the Ph.D. degree from the University of Michigan, Ann Arbor, in 2003.

He was a Control Systems Engineer at Emmeskay, Inc. He has also been a Postdoctoral Research Fellow at the Automated Modeling Laboratory and Automotive Research Center, University of Michigan, where, in May 2006, he joined the Mechanical Engineering Faculty as an Assistant Research Scientist. His current research interests include mechatronic system modeling, system design and control optimization, and automotive systems.